DIGITAL ACCESS TO SCHOLARSHIP AT HARVARD

Coordination of Flagella on Filamentous Cells of Escherichia Coli

(Article begins on next page)

Coordination of Flagella on Filamentous Cells of *Escherichia coli*

AKIRA ISHIHARA, JEFFREY E. SEGALL, STEVEN M. BLOCK, AND HOWARD C. BERG*

Division of Biology, California Institute of Technology, Pasadena, California 91125

Video techniques were used to study the coordination of different flagella on single filamentous cells of *Escherichia coli*. Filamentous, nonseptate cells were produced by introducing a cell division mutation into a strain that was polyhook but otherwise wild type for chemotaxis. Markers for its flagellar motors (ordinary polyhook cells that had been fixed with glutaraldehyde) were attached with antihook antibodies. The markers were driven alternately clockwise and counterclockwise, at angular velocities comparable to those observed when wild-type cells are tethered to glass. The directions of rotation of different markers on the same cell were not correlated; reversals of the flagellar motors occurred asynchronously. The bias of the motors (the fraction of time spent spinning counterclockwise) changed with time. Variations in bias were correlated, provided that the motors were within a few micrometers of one another. Thus, although the directions of rotation of flagellar motors are not controlled by a common intracellular signal, their biases are. This signal appears to have a limited range.

Escherichia coli is propelled by about six flagellar filaments arising at random points on the surface of the cell. Each filament is powered by a rotary motor at its base (7, 28). When the motors turn counterclockwise (CCW), the filaments work together in a bundle that drives the cell steadily forward—the cell runs; when the motors turn clockwise (CW), the bundle flies apart, and the motion is highly erratic—the cell tumbles (20, 23). Runs and tumbles occur in an alternating sequence, each run constituting a step in a three-dimensional random walk (8). When the cell swims in a spatial gradient of a chemical attractant, runs up the gradient are extended; this imposes a bias on the random walk that carries the cell in a favorable direction (8, 22). Changes in concentration of attractants are sensed by specific receptors (1). CCW rotation is favored as more attractant is bound (9, 31). The bias of the flagellar motors (the fraction of time spent spinning CCW) increases in proportion to the rate of change of receptor occupancy (11). The nature of the signal that controls the direction of flagellar rotation is not known.

Is this signal a global signal? Do different flagellar motors on the same cell reverse synchronously? This assumption is implicit in a model, developed extensively by Koshland (17–19), in which CCW and CW rotational states are determined according to whether the value of an intracellular response regulator is above or below some critical value. Transitions between states occur in the absence of chemotactic stim-

ulation, because the regulator (or the critical value) is subject to statistical fluctuation.

An alternative hypothesis asserts that the flagellar motors exist as two-state systems, one state generating CCW rotation and the other CW rotation, with transitions between states governed by first-order rate constants (10, 15). These transitions occur spontaneously, with probabilities that depend on the level of the chemotactic signal. The chemotactic signal affects the bias of the motor, not the particular times at which transitions occur. The motors are autonomous; a correlation should exist between the biases of different flagellar motors but not between their directions of rotation.

The experiments described here were designed to determine whether the motors are autonomous. We grew long, filamentous cells and attached inert, asymmetric markers to their flagella. The markers spun alternately CCW and CW. Transitions between CCW and CW modes occurred asynchronously, whereas variations in bias were correlated, as predicted by the two-state model.

This work confirms and extends that of Macnab and Han (21), who observed asynchronous motion of flagellar filaments on cells of *Salmonella typhimurium* of normal size (nonchemotactic mutants with a strong CW bias observed under conditions of reduced proton motive force). They argued that the asynchrony could be explained by a two-state model or by a response regulator mechanism, provided in the

latter case that fluctuations occur locally, i.e., in a different manner at each flagellar motor. However, as shown elsewhere (11), any threshold-crossing mechanism would be expected to generate CCW and CW interval distributions with many long events, whereas the distributions that are observed are exponential and do not show such events. Again, this behavior is predicted by the two-state model (10, 11).

If the flagellar motors are autonomous, how are their filaments able to work synchronously in a bundle? Which sets of motor states are occupied when cells run or tumble? This problem is discussed in an appendix.

MATERIALS AND METHODS

Strains. All strains were derivatives of *E. coli* K-12. Strain AW405 (wild type) was the gift of J. Alder (24); MS778 (*flaI*, no flagellar structures), YK4105 (*flaE*, polyhooks), and YK4106 (*hag*, no flagellar filaments) were gifts of M. Simon (16, 29, 30, 32); and TOE1 (*ftsQ*, normal growth at 30°C but no septa at 42°C) was the gift of K. J. Begg (4). HB174 (chemotactic at 42°C) was a derivative of AW405 picked from the edge of a tryptone swarm plate at 42°C; wild-type cells grown at this temperature have few flagella (2). HB9 (*flaE hag*) and HB162 (*flaE hag ftsQ*) were constructed from AW405 by P1 cotransduction with *his* or *leu*. HB203 (*flaE hag ftsQ*, chemotactic at 42°C) was constructed in a similar manner from HB174.

Reagents and buffers. All solutions were prepared from reagent-grade chemicals and glass-distilled water. Chloramphenicol, lysozyme (egg white, crystallized three times), and cephalexin were purchased from Sigma Chemical Co. Poly-D-lysine (molecular weight, 151,700) and glutaraldehyde (E.M. grade, 8%) were obtained from U.S. Biochemical and Polyscience, respectively. Rabbit anti-hook antibody was prepared against isolated polyhooks and preadsorbed with cells of strain MS778. Tethering buffer was 90 mM NaCl–10 mM KCl–10 mM potassium phosphate (pH 7.0)–0.1 mM EDTA.

Preparation of filamentous cells. Filamentous cells were prepared in three different ways. Strain HB9 was grown at 35°C in tryptone broth (Difco Laboratories) until early exponential phase, cephalexin (a β-lactam antibiotic) was added (50 μg/ml), and the cells were grown at the same temperature for another 2 h (13, 26). Strain HB162 was grown at 33°C in tryptone broth until early-exponential phase and then shifted to 42°C and grown for 30 min. Strain HB203 was grown at 30°C in tryptone broth until early exponential phase and then shifted to 42°C and grown for 1.5 or 2 h. In all cases, chloramphenicol was added (100 μg/ml), and the cultures were held at their final temperatures for another 20 min; this prevented formation of septa when strains carrying the *ftsQ* mutation were cooled to room temperature.

Preparation of spheroplasts. Spheroplasts were prepared from filamentous cells of strain HB162 and HB203 by a method adapted from Onitsuka et al. (25). Cells were washed twice with 50% sucrose (wt/vol) and resuspended in the same solution. Lysozyme and EDTA were added to final concentrations of 0.09 mg/

ml and 12 mM, respectively. The suspension was incubated at 37°C for 10 min and diluted 10-fold with Penassay broth (Difco).

Preparation of markers. Strain HB9 was grown at 35°C in tryptone broth. The cells were treated with 0.1% glutaraldehyde for 30 min, washed three times with tethering buffer, and resuspended in the same buffer (about 10^10 cells per ml).

Tethering. Markers were attached to filamentous cells that were fixed to a cover slip with poly-D-lysine. The cover slip was dipped in poly-D-lysine (0.2 mg/ml) and air dried. It was then sealed at opposite edges to two other cover slips (0.15 mm thick) greased to a glass slide (all with Apiezon L) to form a flow chamber with a volume of about 50 μl. When solutions were added to the chamber, it was held cover slip up, and the eluent was taken up with a piece of filter paper. Otherwise, it was placed upside down on spacers in a wet petri dish. Fifty microliters of culture medium was added, and the filamentous cells were allowed to settle for 20 min. Then, 50 μl of anti-hook antibody (preadsorbed antisera diluted about 1:500 with tethering medium) was added, and the mixture was allowed to stand for 1 h. Next, 30 μl of the marker suspension was added, and the mixture was allowed to stand for 30 min. Finally, the assembly was turned right-side up and placed on the microscope stage for observation.

Data acquisition and analysis. The motion of the markers was recorded on videotape by inverse phase-contrast microscopy with a Nikon Optiphot microscope (Plan 40 BM objective, Photo 8× eyepiece), a Sanyo VC1620X video camera, and a Sanyo VTC7100 cassette recorder. In some experiments, the temperature of the stage and objective were controlled at 22°C with an aluminum block coupled to a water-cooled Peltier element (14a). A digital time display was included in the recording. It was pulsed from black to white once every 45 s as an additional timing signal (see below).

The videotapes were played back at one-quarter speed. An operator scored the directions of rotation of the markers by eye, depressing or releasing a pushbutton that tripped a pen on a strip-chart recorder (11). A photodiode placed on the screen over the time display tripped a second pen when this display changed from black to white. This made it possible for records obtained with different markers to be synchronized and for slippage of the charts that occurred in readings of long records to be corrected. The strip charts were digitized (10), and the data, a list of numbers representing the time of CW-to-CCW and CCW-to-CW transitions, were analyzed with a PDP 11/34 computer. The cumulative error in the timing of events was less than 0.3 s, based on errors arising from operator response time (about 0.1 s) and from slippage of the chart paper while digitizing segments of length 45 s (about 0.2 s).

Pairs of records, designated $x(t)$ and $y(t)$, each of length T, were considered as a function of time and assigned the value +1 whenever the marker spun CCW and −1 whenever it spun CW. The direction correlation function, the time average $<x(t)y(t + \tau)>$, provides a measure of interrelation between the rotational sense of the two records at any lag (or lead) time, τ (5). This function was computed by dividing T into equal time intervals, δt (generally 0.2 s), and computing the average:

$$\frac{1}{N} \sum_k x(k\delta t)y(k\delta t + \tau) \qquad (1)$$

where, for $\tau > 0$, k ranged from 0 to $N = (T - \tau)/\delta t$, and for $\tau < 0$, k ranged from $-\tau/\delta t$ to $T/\delta t$; τ assumed values that were integral multiples of δt. When the two records computed were the same, i.e., when $x(t) = y(t)$, we obtained the direction autocorrelation function, which decays from 1 at zero lag—since $x(t)$ is either $+1$ or -1, its mean square value is 1—to an asymptotic value at infinite lag equal to the square of the mean value of $x(t)$. When transitions between rotational states occur at random, this decay is exponential, with a time constant equal to the reciprocal of the sum of the rates of transition between the two states. Computation of the direction correlation function enables systematic interrelations between different markers to be detected, even if the two markers do not reverse simultaneously, but do so with a relative lag, and even if reversals are not coupled with very high probability.

The rotational bias of a marker, defined as the fraction of time that it spins CCW, was computed over periods of 20 s. A running average, made in steps of 2 s, provided a smoothed estimate of the bias over the complete record. Bias correlation functions were computed in the same way as direction correlation functions (using $\delta t = 2$ s), except that the mean bias for each marker was first subtracted out; i.e., the relative biases $x(t) - <x>$ and $y(t) - <y>$ were used.

The means and standard deviations in direction or bias correlation expected for a given pair of markers, assuming that they were not cross-correlated, were estimated by using a Monte Carlo method. Thirty pairs of simulated records were constructed by a random-number process that generated exponential distributions of CCW and CW intervals. The mean CCW and CW intervals were chosen to match those measured for the pairs of markers under study. These data were analyzed in the same way as the real data, and standard deviations were estimated from the scatter in the 30 direction or bias correlation functions. To determine the extent to which a bias correlation was statistically significant, a bias correlation ratio was computed by dividing the amplitude of the correlation of the real markers at zero lag by the standard deviation in this quantity obtained from the simulation. A bias correlation ratio of 4.0 or greater indicates a high degree of synchronization near zero lag.

The angular velocities of the markers were measured by playing the video tapes back at one-quarter speed and timing 10 revolutions with a stop watch. This measurement was repeated several times during the course of each experiment.

RESULTS

Markers rotated when on filamentous cells.
The markers, cells of strain HB9 fixed with glutaraldehyde, were inert when attached to glass, but they spun when attached to the filamentous cells. Thus, torque was generated by the filamentous cells, not by the markers. To learn whether the markers might contaminate the preparation in some way, we exposed wild-type cells tethered to glass to a suspension of

markers at a density of about 10^{10} cells per ml. No changes were observed in the behavior of the tethered cells. The markers were much shorter than the filamentous cells, so there was no problem in distinguishing the two (Fig. 1). The lengths of the filamentous cells used in this study ranged from 20 to more than 120 μm (Table 1, column 2).

The filamentous cells did not adhere strongly to the cover slip; therefore, some markers were free to rotate even when attached to the sides of a cell (Fig. 2). The markers rotated alternately CCW and CW, at angular velocities comparable to those observed when wild-type cells are tethered to glass (Table 1, columns 5, 7, and 8). The CCW intervals tended to be longer than those observed with wild-type cells (9, 11), yielding somewhat higher biases (Table 1, column 6), but the angular velocities fell in a comparable range, with short markers (or short wild-type cells) rotating more rapidly than long markers (or long wild-type cells). As many as three markers were followed on a single cell (Table 1, experiments 7 and 8). The records for the last 134 s of experiment 8 are shown in Fig. 3.

The filamentous cells responded to temperature shifts and to chemotactic stimuli. Adaptation occurred in either case. The markers spun CCW for a time when the cells were heated and CW when they were cooled. They spun CCW when the cells were exposed to aspartate, delivered iontophoretically (27). In many cases, it was difficult to tell whether a marker was attached to the near side or the far side of a filamentous cell. In experiments 8 through 14, thermal responses were used to verify directions of rotation. In experiments 1 through 7, the determination was made by assuming that the bias was greater than 0.5. Errors made in this
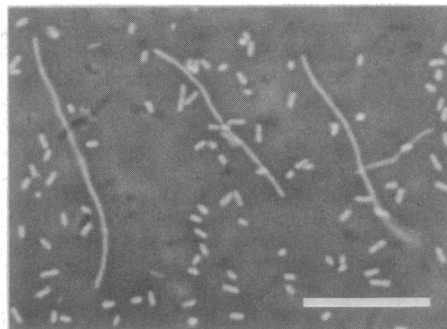

FIG. 1. Filamentous cells of strain HB203 mixed with glutaraldehyde-fixed cells of strain HB9 in the presence of anti-hook antibody. The filamentous cells picked up 0, 2, 1, and 1 markers, respectively (left to right). The plane of focus was near the surface of the cover slip. Most of the markers were attached to glass. Bar, 20 μm.

could be seen along the filamentous cells. Spheroplasts of these cells consisted of clusters of small spheres. Thus, the presence of septa could be determined visually. No septa were seen between any of the markers included in this study.

Dramatic evidence for the continuity of the cytoplasmic space was obtained in experiment 8 when the three markers (Fig. 2) slowed down over an interval of about 1.5 s and stopped, coming to rest within about 0.1 s of one another (Fig. 3, arrow). About 1 min later, the markers began to rotate again, starting up slowly and reaching their original speeds after about 1.5 min. They started CCW and continued to spin in this direction for about 20 s after reaching top speed before switching back and forth between the CW and CCW modes. This behavior is consistent with the sudden collapse and gradual restoration of proton motive force that would be expected if a hole were to open up and close in the cytoplasmic membrane. This was a rare event; all of the other markers that we observed rotated continuously.

Motors on the same cell changed directions asynchronously. When records for different markers on the same cell were placed in register, as in Fig. 3, no synchronization was apparent. This was confirmed by computing the direction correlation function, as described above. Figure 4 compares the direction autocorrelation function for marker A of experiment 1 with the direction cross-correlation function for markers A and B. There was no correlation at any lag between any of the pairs of markers in Table 1 greater than that expected by chance, assuming that each motor changed directions at random (allowing for the slow drifts in bias described below).

Biases were not constant. Different motors on the same cell tended to have similar biases (Table 1, column 6), but this also was true for motors on other cells in the same preparation (compare the biases of markers labeled X). Larger differences occurred from preparation to preparation.
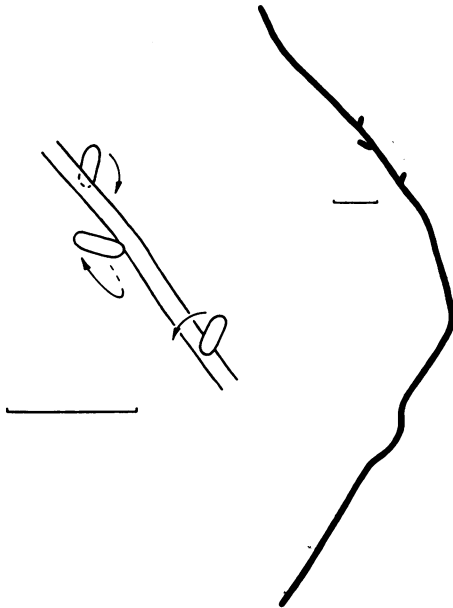

FIG. 2. Tracing from the video screen of a filamentous cell of strain HB203 carrying three markers (Table 1, experiment 8). The markers are shown in the inset (enlarged ×3) at a time when each was rotating CCW. Marker A (top) was on the far side of the filamentous cell, marker B (middle) on the left side, and marker C (bottom) on the near side, between the filamentous cell and the cover slip. Each bar, 5 μm.

way, if any, affect the signs of correlation calculations, not their amplitudes.

Filamentous cells had a single cytoplasmic space. Spheroplasts were prepared from filamentous cells of strains HB162 and HB203. When the cells were grown at 42°C, preparations with long cells gave large spheres, and preparations with short cells gave small spheres. For example, filamentous cells about 40 μm long gave spheres about 4 μm in diameter, and cells about 3 μm long gave spheres about 1 μm in diameter. This indicates that the cytoplasmic space was enclosed by one continuous membrane. When these strains were grown at 35°C, many septa
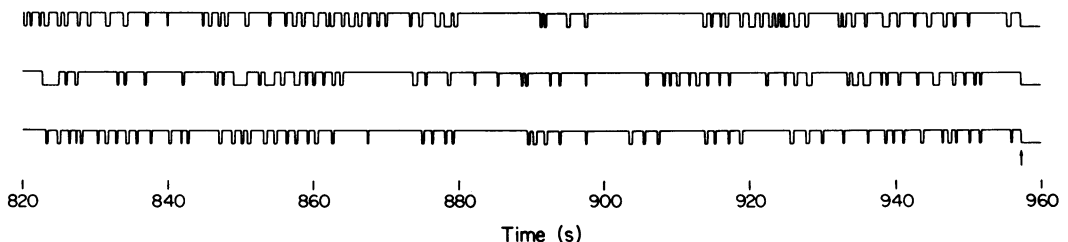

FIG. 3. Strip-chart records for markers A (top), B (middle), and C (bottom) of Fig. 2 (CCW direction, up; CW direction, down) for the last 134 s of experiment 8. The markers stopped within about 0.1 s of one another at the point shown by the arrow.
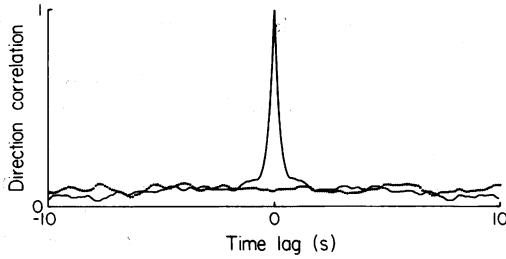
FIG. 4. Direction autocorrelation function for marker A of experiment 1 (solid curve) and the cross-correlation function for markers A and B of experiment 1 (dotted curve), shown for time lags ranging from −10 to +10 s.

Variations in bias of a given motor were examined by computing a running average. These functions fluctuated in a manner expected for averages of two-state systems that change states at random, as shown in the bottom panel of Fig. 5, but in some cases, as shown in the top panel, the variations in bias were larger than expected and occurred over a longer time span. Precise temperature control was introduced in experiments 8 through 14 in an attempt to reduce these variations, but without effect. The variations in bias were not due to changes in proton motive force because the angular velocities of the motors remained constant (15). For example, 50 measurements were made of the angular velocities of each of the markers whose biases

TABLE 1. Properties of the filamentous cells used in this study[a]

Expt. no.	Cell length (μm)	Data length (s)	Marker label[b]	Angular velocity (Hz)	Bias[c]	Mean interval		No. of CCW and CW events	Marker separation (μm)	Bias correlation ratio
						CCW (s)	CW (s)			
1	>80	891	A	3.6	0.59	0.83	0.56	1,283	14	5.6
			B	4.8	0.65	2.12	1.16	544		
2	66	166	A	7.6	0.71	1.38	0.59	168	6	0
			B	6.5	0.77	2.93	0.87	87		
3[d]	95	366	A	4.7	0.75	1.11	0.37	496	6	8.8
			B	6.8	0.70	0.97	0.41	533		
4[d]	20	163	A	7.1	0.75	2.71	0.95	89	6	1.2
			B	ND[e]	0.59	2.19	1.56	87		
5	60	385	A	10.2	0.84	5.24	0.99	123	18	2.6
			B	9.4	0.85	4.50	0.79	145		
6	>120	377	A	3.8	0.83	2.56	0.52	244	5	4.7
			B	4.1	0.84	2.82	0.54	223		
7[f]	34	703	A	2.4	0.67	1.97	0.96	479	5 (AB)	7.1
			B	6.1	0.85	4.01	0.71	297	16 (BC)	2.0
			C	6.8	0.93	5.89	0.44	222	21 (AC)	0.3
8	80	954	A	9.3	0.82	3.88	0.83	405	3 (AB)	7.9
			B	2.8	0.83	3.94	0.81	402	5 (BC)	5.8
			C	7.2	0.90	5.33	0.60	322	8 (AC)	4.3
9	80	207	A	2.8	0.84	2.99	0.58	116	3 (AB)	4.0
			B	8.0	0.88	10.2	1.41	35	25 (BX)	−0.3
			X	1.4	0.93	12.9	0.98	29	23 (AX)	−0.1
10	100	405	A	9.8	0.29	1.05	2.57	224	47	−0.3
			B	4.5	0.09	1.08	11.2	65		
11	45	787	A	ND	0.95	24.3	1.14	62	11 (AB)	1.6
			B	ND	0.91	6.58	0.64	218	4 (BX)	−3.4
			X	ND	0.97	19.1	0.58	78	11 (AX)	−0.5
12	54	278	A	3.7	0.83	7.18	1.49	64	8 (AB)	0.8
			B	3.6	0.83	2.30	0.48	199	8 (BX)	0.1
			X	2.5	0.87	7.35	1.10	65	4 (AX)	−1.7
13	55	252	A	ND	0.41	0.79	1.15	260	30	−2.8
			B	7.6	0.47	1.42	1.58	168		
14	37	474	A	4.0	0.65	2.19	1.17	281	9	0.8
			B	6.9	0.59	1.15	0.79	488		

[a] Cells of strain HB203 grown at 42°C in tryptone broth, except as noted. The experiments were done at room temperature (22°C), with precise temperature control for experiments 8 through 14.
[b] A, B, and C indicate markers on the same cell, and X indicates a marker on a second nearby cell.
[c] The fraction of time spent spinning CCW.
[d] Strain HB162 grown at 42°C in tryptone broth.
[e] ND, Not determined.
[f] Strain HB9 grown at 35°C in tryptone broth in the presence of cephalexin.
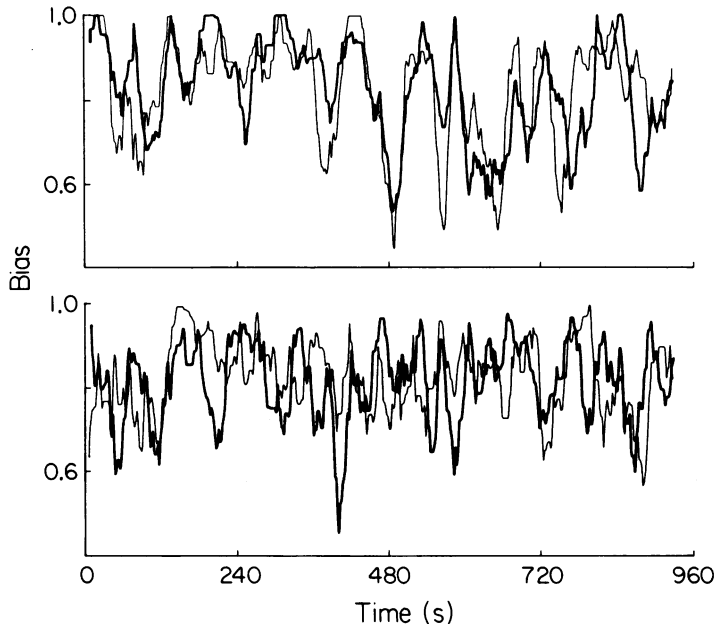
FIG. 5. (Top) Biases of markers A (thick curve) and B (thin curve) of experiment 8. (Bottom) Biases of two simulated markers with the same mean biases as markers A and B.

are shown in the top panel of Fig. 5 over a 130-s interval centered at 480 s, an interval during which the biases varied by as much as 50%. No deflections in angular velocity were apparent (mean ± 1 standard deviation, 9.3 ± 0.7 and 2.8 ± 0.2 Hz, respectively).

Some biases were correlated. Another feature apparent in the data shown in the top panel of Fig. 5 is that the biases of the two motors rose and fell synchronously. This was confirmed by computing the bias correlation function, with the results shown in Fig. 6. The bias correlation ratio, defined above, was 7.9 for experiment 8 (Table 1, last column). This value indicates a high degree of correlation between the biases of the motors at zero lag. A scatter plot of bias correlation ratio as a function of motor separation is shown in Fig. 7. There was a clear correlation for some, but not all, motors separated by 10 μm or less. In experiments 7 and 8, in which three markers were attached to each cell, the correlation decreased with distance. None of the markers on different cells were correlated, even when these markers were close to one another. We conclude that variations in the bias of the flagellar motors can be correlated, provided that the motors are on the same cell and no more than a few micrometers apart.

DISCUSSION

In summary, we attached markers to different flagellar motors on single filamentous cells (Fig.

1 and 2, Table 1). The cells responded to chemical and thermal stimuli. They were fully energized, as judged by speed and direction of flagellar rotation, and they contained a single cytoplasmic space, as judged by the formation of giant spheroplasts and by a fortuitous event in which three adjacent markers stopped synchronously (Fig. 3, arrow). The markers were far enough apart that they did not interact mechanically. We were unable to find any correlation in the directions of rotation of different flagellar motors (e.g., Fig. 4, dotted curve). The biases of the motors shifted with time (e.g., Fig. 5, top
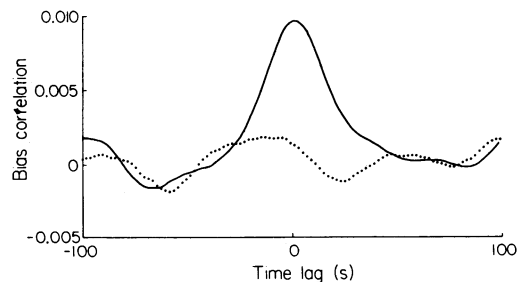
FIG. 6. Bias correlation functions for the data shown in the top and bottom panels of Fig. 5 (solid and dotted curves, respectively) for time lags ranging from −100 to +100 s. The standard deviation in bias correlation expected for uncorrelated markers was ±0.0012 (not shown).

FIG. 7. Bias correlation ratio as a function of marker separation for pairs of markers on the same cell (closed symbols) or on different cells (open symbols). Three markers were observed on the same cell in experiments 7 (■) and 8 (▲).

panel). The biases of different motors tended to shift in synchrony, provided that the motors were on the same cell and within a few micrometers of one another (Fig. 6 and 7).
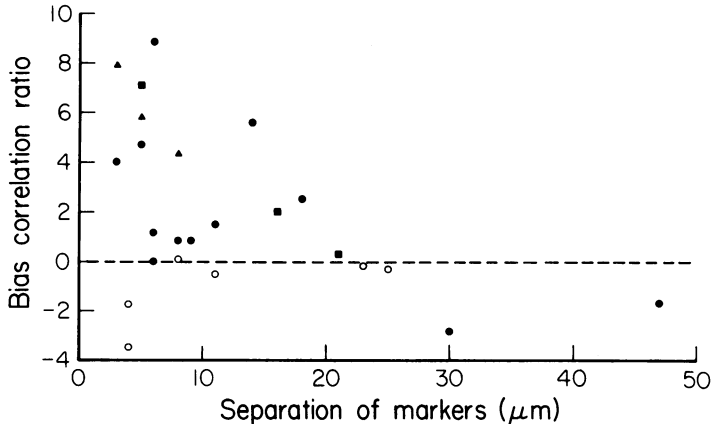
A global signal does not synchronize flagellar motors. The absence of direction correlation at any lag shows that the times at which flagellar reversals occur are not subject to coordinate control. If such control were exerted either chemically or electrically on motors, say, 3 μm apart (the closest pairs examined), coordination would be expected on time scales of milli- or microseconds, respectively. The time required for a motor to change the direction of rotation of a tethered cell once a reversal is initiated is 10 ms or less (6), so this delay is not important. The possibility that coordination occurs when motors are closer to one another than 3 μm is ruled out by the data of Macnab and Han (21), who observed asynchronous reversals of flagellar filaments on single cells of S. typhimurium. However, their experiments are not strictly equivalent to ours, because they used mutants with an extreme CW bias under conditions of reduced proton motive force. This allowed reversals to occur at torques below those that generate polymorphic transitions (23). The motors of their cells frequently stopped, a behavior not observed here. Whether this was due to the reduced proton motive force, to mechanical interactions between different flagellar filaments, or to interactions between these filaments and the glass is not known.

A global signal does control motor bias. Although transitions between CCW and CW states occur at random times, the rates at which these transitions occur are subject to coordinate control. This is shown by the strong bias correlation between some motors on the same cell (as

represented by the points in the upper left-hand corner of Fig. 7). The reasons for the changes in bias leading to this correlation are not known. These changes were not due to drifts in external variables, such as temperature, because there was no bias correlation between markers on different cells. Note, in experiments 8 through 14, that the correlation persisted when the temperature was carefully controlled.

This signal has a finite range. The fact that the bias correlation was strongest for motors only a few micrometers apart indicates that the signal has a finite range, long compared to the length of a normal cell but short compared to the length of a filamentous cell. If the signal is electrogenic and the filamentous cell has cable properties similar to those of a nerve axon of the same diameter, then a space constant for potential of several hundred micrometers is expected (3). Thus, an electrogenic signal seems unlikely, but it cannot be ruled out. If the signal is some chemical, then it must be inactivated or removed from the cell. It is not able to equilibrate over distances much larger than about 10 μm in times less than about 1 min, the time scale on which the variations in bias occurred. Note that a small molecule can diffuse 10 μm in water in about 0.1 s.

Flagellar motors function as two-state systems. These results argue for a two-state model (10), in which a motor exists either in a state that generates CCW rotation (runs) or in a state that generates CW rotation (tumbles). Transitions between these states are governed by first-order rate constants, which are the probabilities per unit time that the occupation of a state is terminated. These are the parameters that are subject to global control.

An alternative hypothesis asserts that transitions are generated by threshold crossings of a

signal subject to statistical fluctuation (17–19). The lack of synchronization could be explained in this model if fluctuations were local rather than global (21), especially if they occurred in the threshold rather than in the signal, since the thresholds could be set independently at each motor. However, as shown elsewhere (11), threshold-crossing mechanisms lead to CCW and CW interval distributions with extended tails, i.e., with relatively large numbers of long events. The CCW and CW interval distributions observed experimentally are exponential; they do not show these events (11). Exponential distributions are the hallmark of two-state systems.

We do not know how transitions between rotational states are generated. They could occur through changes in protein conformation, through the binding and unbinding of a ligand at a receptor, or the like. If so, the signal affects the stabilities of alternate conformations, the on and off rate constants, or the like. It does not generate the transitions per se.

Discrepancies between run/tumble and CCW/CW statistics remain unresolved. If the flagellar motors are autonomous, how do their filaments work synchronously in a bundle? In *E. coli* strain AW405, the mean run and tumble lengths are about 1 and 0.1 s, respectively (8), whereas the mean CCW and CW intervals are both about 1 s (9, 11). As discussed in the Appendix, one possibility is that a cell runs when half or more than half of its filaments rotate CCW and tumbles otherwise. However, the fit to the data is not very good. A more elaborate mechanism seems to be required.

APPENDIX

Voting hypothesis. If the motors driving the flagellar filaments reverse independently, and therefore asynchronously, how does a flagellar bundle form to allow a concerted run in one direction? The simplest possibility is that a stable bundle is formed when a certain fraction (e.g., greater than or equal to one-half) of the motors rotate in the CCW direction. Once the bundle is formed, individual filaments whose rotational sense does not coincide with the majority (i.e., those trying to spin CW) are driven against their preferred rotational sense, and the bundle remains stable. When a sufficient number of flagella have, by chance, changed their preferred sense of rotation from CCW to CW (so as to reduce the number CCW below the fixed fraction required for stability), the bundle flies apart, and the cell tumbles. According to this hypothesis, the overall state of the several individual motors determines whether the cell runs or tumbles. This possibility will be referred to as the "voting hypothesis," in that independent flagella vote upon whether the cell is in the run or tumble mode by attempting to turn CCW or CW, respectively. The fraction required for a stable run, i.e, the "rules" for determining what constitutes a majority, remains to be determined. A version of this

hypothesis was first advanced by Khan and Macnab (15), who suggested that a tumble might be initiated when more than one flagellum in a bundle tried to reverse. However, their assumption that the system can be treated as if at steady state is not valid, so that the run times that they were led to predict are in error.

Predictions of the voting hypothesis. The voting hypothesis assumes that individual flagella are completely autonomous; each is endowed with a set of switching probabilities for transitions between CCW and CW states. Once these probabilities are known, then it is possible to derive an expression for the length of time during which a number n or more of f flagella are trying to rotate CCW. Such an expression is obtained below; it defines the mean run and tumble times for a cell in terms of the mean CCW and CW intervals of the separate motors.

For wild-type *E. coli*, mean run times are about 1.1 s (0.86 s adjusted upward by the 0.24-s interval required to detect a run; see reference 8, addendum), whereas mean tumble times are about 0.14 s. A swimming cell therefore spends almost 90% of the time running. When tethered, however, individual flagellar filaments spend nearly equal amounts of time rotating in the CCW and CW directions (9). For the wild type, mean CCW times are about 1.20 s, whereas mean CW times are about 1.06 s (11). All of these values were obtained with cells of the same wild-type strain in similar media at the same temperature (strain AW405 in dilute phosphate buffer at 32°C). We assume that cells of *E. coli*, like those of *S. typhimurium* (14), have, on average, about six flagella.

Are these figures consistent with the predictions of the voting hypothesis? The results of computations given in Table 2 and discussed below suggest that they are not; the observed tumble times are too short to be accommodated by the voting hypothesis, given the measured values for mean rotational times. Conversely, given the measured values for run and tumble times, one is led to predict mean CW intervals that are much shorter than those generally seen. Similar results were obtained in computations assuming numbers of flagella ranging from four to nine. The possibility remains that the published values are inconsistent because of the way in which the cells were selected for study, but we view this as unlikely.

In addition, the voting hypothesis would require runs and tumbles to be distributed as sums of several exponential processes, whereas experimental evidence indicates that runs and tumbles are distributed as single exponentials (8), just as are CCW and CW intervals (11). Under certain conditions, sums of exponentials can be difficult to distinguish from pure exponentials, but again we view this possibility as unlikely. Although mean run times have a large biological variability in swimming cells, mean tumble times are remarkably constant (8). On the other hand, both mean CCW and CW intervals show variability in tethered cells. This asymmetry is not easily explained by the voting hypothesis.

The voting hypothesis also predicts that the torque produced by a rotating bundle should vary with time, as the number of flagella asserting CCW rotation within the bundle changes. Under conditions in which torque is limiting, e.g., in a medium of high viscosity, changes in torque will be reflected in changes in angular velocity, so one would expect to see fluctua-

TABLE 2. Predicted run and tumble times for the voting hypothesis[a]

Case	Minimum no. of flagella required to be in CCW mode for a run	Predicted mean run time (s)	Predicted mean tumble time (s)
1[b]	1	16.42	0.18
	2	2.69	0.24
	3	**0.92**	**0.37**
	4	0.46	0.68
	5	0.29	1.74
	6	0.20	8.72
2[c]	1	553.52	0.07
	2	31.55	0.08
	3	4.41	0.11
	4	**1.12**	**0.17**
	5	0.44	0.29
	6	0.23	0.82

[a] The numbers shown in boldface provide the closest match of observed and predicted interval times. The calculations assume six flagella per cell.

[b] In this case, we assume a mean CCW interval of 1.20 s and a mean CW interval of 1.06 s (measured values, see the text).

[c] In this case, we assume a mean CCW interval of 1.4 s and a mean CW interval of 0.4 s (values adjusted to give prediction of times close to the measured values for the mean run and tumble times, see the text).

tions in the speed of swimming cells. Preliminary measurements of the speeds of swimming cells in a medium containing 9.5% Ficoll (4.0 cP) do not show such fluctuations (J. E. Segall, unpublished data). Therefore, it appears unlikely that the voting hypothesis, in the simple form presented here, is correct. More complicated voting rules seem to be required. For example, when a flagellum is outvoted, it might simply change its vote. Mechanical interactions between flagellar filaments, acting through some kind of feedback process, might cause the motor to assert the opposite torque. But tethered cells do not reverse direction when their rotation is suddenly blocked by a micropipette or when they become stuck briefly on the tethering surface (M. D. Manson and S. M. Block, unpublished data). However, this observation does not rule out the possibility of feedback under conditions of less limiting torque. Somehow, tumbles are terminated prematurely. Too little is known at present about the interactions of flagellar filaments to explain the disparity between run/tumble interval times and CCW/CW interval times.

Mathematics of the voting hypothesis. A cell with f flagella can exist in $(f + 1)$ states, ranging from $n = 0$ up to $n = f$ flagella rotating CCW at any instant. Assuming that the rates for CCW-to-CW and for CW-to-CCW transitions are the same for all the flagella and equal to k_r and k_t, respectively, we have the system:

$$[0] \underset{k_r}{\overset{fk_t}{\rightleftharpoons}} [1] \underset{2k_r}{\overset{(f-1)k_t}{\rightleftharpoons}} \cdots \underset{nk_r}{\overset{(f-n-1)k_t}{\rightleftharpoons}} [n] \underset{(n+1)k_r}{\overset{(f-n)k_t}{\rightleftharpoons}}$$

$$[n+1] \underset{(n+2)k_r}{\overset{(f-n+1)k_t}{\rightleftharpoons}} \cdots \underset{fk_r}{\overset{k_t}{\rightleftharpoons}} [f] \quad (2)$$

where the states represent various numbers of flagella asserting the CCW direction. If the critical number of flagella spinning CCW is n or more, then run times will correspond to the lifetime of the compound state consisting of all individual states greater than or equal to n. The complete system can be solved as a set of $f + 1$ coupled differential equations (an eigenvalue problem); the solution for the compound (run) state, above, will consist of a weighted sum of $f - n + 1$ exponentials, whereas the solution for the companion compound (tumble) state will consist of a weighted sum of n exponentials. The problem can be solved by standard methods (cf. reference 12). However, a simple recursion relationship can be developed to obtain the lifetime of each state by using the theory of the random walk. One obtains for the mean time for passage from the state n to the $n + 1$st state:

$$t_{(n, n+1)} =$$

$$[k_{(n,n-1)}/k_{(n,n+1)}]t_{(n-1,n)} + 1/k_{(n,n+1)} \quad (3)$$

where the k values are the transition rate constants among the subscripted states. The lifetime of the 0th state is simply $1/k_{(0,1)}$. Lifetimes for other states are obtained by recursion. Experimentally determined mean CCW and CW interval times give the reciprocals for k_r and k_t in equation 2. Using these values, and assuming six flagella per cell, we obtain the results shown in Table 2. If the rules for the voting hypothesis are such that half or more of the flagella are required to assert the CCW direction for a run to occur, we obtain run and tumble times of 0.92 and 0.37 s, respectively (Table 2). Although the run time agrees reasonably well with the observed mean run length of 1.1 s, the tumble time differs by almost a factor of three; 0.37 s is predicted whereas the measured value is 0.14 s. To get values close to the measured run and tumble times, we are forced to assume a mean CCW interval of 1.4 s and a mean CW interval of 0.4 s (Table 2).

Derivation of equation 3. The coupled system in equation 2 can be viewed as a random walk among states, with transition probabilities whose values depend upon the number of the state. We seek a mean time to passage across a boundary between state n and state $n + 1$. Let P_m be the probability that the system moves from state n to state $n - 1$ exactly m times before stepping from n to $n + 1$. Let T be the waiting time in the nth state before a step. T will be given by the reciprocal of the sum of the rate constants leaving the state, i.e., by:

$$T = 1/[k_{(n,n-1)} + k_{(n,n+1)}] \quad (4)$$

The mean waiting time for a cell in state n to move to the $(n + 1)$st state is given by:

$$t_{(n,n+1)} = \left\{ \sum_m mP_m[t_{(n-1,n)} + T] \right\} + T \quad (5)$$

Let p be the probability of a step from n to $n - 1$. Then:

$$P_m = p^m(1 - p) \qquad (6)$$

where $p = k_{(n,n - 1)}/[k_{(n,n - 1)} + k_{(n,n + 1)}]$. Substituting this expression into equation 5 and summing over all m gives:

$$t_{(n,n + 1)} = \frac{p}{1 - p}[t_{(n - 1,n)} + T] + T \qquad (7)$$

Further substitution of the expression for p in terms of the rates k gives equation 3. A similar recursion expression can be derived for transitions from a higher to a lower state. All rate constants for transitions to higher states will be multiples of k_t, whereas all rate constants for transitions to lower states will be multiples of k_r, the multiplicity being determined by the number of flagella rotating CCW.

LITERATURE CITED

1. Adler, J. 1969. Chemoreceptors in bacteria. Science 166:1588–1597.
2. Adler, J., and B. Templeton. 1967. The effect of environmental conditions on the motility of Escherichia coli. J. Gen. Microbiol. 46:175–184.
3. Aidley, D. J. 1978. The physiology of excitable cells, 2nd ed, p. 47–53. Cambridge University Press, Cambridge.
4. Begg, K. J., G. F. Hatfull, and W. D. Donachie. 1980. Identification of new genes in a cell envelope-cell division gene cluster of Escherichia coli: cell division gene ftsQ. J. Bacteriol. 144:435–437.
5. Bendat, J. S., and A. G. Piersol. 1971. Random data: measurement and analysis procedures. Wiley-Interscience, New York.
6. Berg, H. C. 1976. Does the flagellar rotary motor step?, p. A47–A56. In R. Goldman, T. Pollard, and J. Rosenbaum (ed.), Cold Spring Harbor Conferences on Cell Proliferation, vol. 3, cell motility. Cold Spring Harbor Laboratory, Cold Spring Harbor, N.Y.
7. Berg, H. C., and R. A. Anderson. 1973. Bacteria swim by rotating their flagellar filaments. Nature (London) 245:380–382.
8. Berg, H. C., and D. A. Brown. 1972. Chemotaxis in Escherichia coli analysed by three-dimensional tracking. Nature (London) 239:500–504. Reprinted with an addendum, 1974, p. 55–78, In E. Sorkin (ed.), Antibiotics and chemotherapy, vol. 19, chemotaxis: its biology and biochemistry. S. Karger, Basel.
9. Berg, H. C., and P. M. Tedesco. 1975. Transient response to chemotactic stimuli in Escherichia coli. Proc. Natl. Acad. Sci. U.S.A. 72:3235–3239.
10. Block, S. M., J. E. Segall, and H. C. Berg. 1982. Impulse responses in bacterial chemotaxis. Cell 31:215–226.
11. Block, S. M., J. E. Segall, and H. C. Berg. 1983. Adaptation kinetics in bacterial chemotaxis. J. Bacteriol. 154:312–323.
12. Colquhoun, D., and A. G. Hawkes. 1977. Relaxation and fluctuations of membrane currents that flow through drug-operated channels. Proc. R. Soc. London Ser. B 199:231–262.
13. Greenwood, D., and F. O'Grady. 1973. Comparison of the responses of Escherichia coli and Proteus mirabilis to seven β-lactam antibiotics. J. Infect. Dis. 128:211–222.
14. Iino, T. 1974. Assembly of Salmonella flagellin in vitro and in vivo. J. Supramol. Struct. 2:372–384.
14a. Khan, S., and H. C. Berg. 1983. Isotope and thermal effects in chemiosmotic coupling to the flagellar motor of Streptococcus. Cell 32:913–919.
15. Khan, S., and R. M. Macnab. 1980. The steady-state counterclockwise/clockwise ratio of bacterial flagellar motors is regulated by protonmotive force. J. Mol. Biol. 138:563–597.
16. Komeda, Y., and T. Iino. 1979. Regulation of expression of the flagellin gene (hag) in Escherichia coli K-12: analysis of hag-lac gene fusions. J. Bacteriol. 139:721–729.
17. Koshland, D. E., Jr. 1977. A response regulator model in a simple sensory system. Science 196:1055–1063.
18. Koshland, D. E., Jr. 1979. A model regulatory system: bacterial chemotaxis. Physiol. Rev. 59:811–862.
19. Koshland, D. E., Jr. 1980. Bacterial chemotaxis as a model behavioral system. Raven Press, New York.
20. Larsen, S. H., R. W. Reader, E. N. Kort, W.-W. Tso, and J. Adler. 1974. Change in direction of flagellar rotation is the basis of the chemotactic response in Escherichia coli. Nature (London) 249:74–77.
21. Macnab, R. M., and D. P. Han. 1983. Asynchronous switching of flagellar motors on a single bacterial cell. Cell 32:109–117.
22. Macnab, R. M., and D. E. Koshland, Jr. 1972. The gradient-sensing mechanism in bacterial chemotaxis. Proc. Natl. Acad. Sci. U.S.A. 69:2509–2512.
23. Macnab, R. M., and M. K. Ornston. 1977. Normal-to-curly flagellar transitions and their role in bacterial tumbling. Stabilization of an alternative quaternary structure by mechanical force. J. Mol. Biol. 112:1–30.
24. Mesibov, R., and J. Adler. 1972. Chemotaxis toward amino acids in Escherichia coli. J. Bacteriol. 112:315–326.
25. Onitsuka, M. O., Y. Rikihisa, and H. B. Maruyama. 1979. Biochemical and topographical studies on Escherichia coli cell surface. IV. Giant spheroplast formation from a filamentous cell. J. Bacteriol. 138:567–574.
26. Robinson, G. N. 1980. Effect of β-lactam antibiotics on bacterial cell growth rate. J. Gen. Microbiol. 120:317–323.
27. Segall, J. E., M. D. Manson, and H. C. Berg. 1982. Signal processing times in bacterial chemotaxis. Nature (London) 296:855–857.
28. Silverman, M., and M. Simon. 1974. Flagellar rotation and the mechanism of bacterial motility. Nature (London) 249:73–74.
29. Silverman, M., and M. Simon. 1974. Characterization of Escherichia coli flagellar mutants that are insensitive to catabolite repression. J. Bacteriol. 120:1196–1203.
30. Silverman, M. R., and M. I. Simon. 1972. Flagellar assembly mutants in Escherichia coli. J. Bacteriol. 112:986–993.
31. Spudich, J. L., and D. E. Koshland, Jr. 1975. Quantitation of the sensory response in bacterial chemotaxis. Proc. Natl. Acad. Sci. U.S.A. 72:710–713.
32. Suzuki, T., and Y. Komeda. 1981. Incomplete flagellar structures in Escherichia coli mutants. J. Bacteriol. 145:1036–1041.